RELAXING CONSERVATISM OF ROBUST DISTURBANCE OBSERVER BASED TORQUE CONTROL OF SERIES-ELASTIC ACTUATORS FOR ARTICULATED ROBOTS

L. (Luuk) Lomillos Rozeboom

MSC ASSIGNMENT

Committee:
prof. dr. ir. S. Stramigioli
dr. ir. W. Roozing
dr. ir. R.G.K.M. Aarts

March, 2021

013RaM2021
Robotics and Mechatronics
EEMCS
University of Twente
P.O. Box 217
7500 AE Enschede
The Netherlands

UNIVERSITY OF TWENTE. | TECHMED CENTRE
UNIVERSITY OF TWENTE. | DIGITAL SOCIETY INSTITUTE

Abstract

The use of series elastic actuators for torque control of articulated robots has seen an increase in adoption in the last years due to some clear benefits with respect to conventional actuators. The dynamic behaviour of articulated robots is highly nonlinear. Two different controller design methods are investigated in this paper. The first one defines the control design as an optimization problem with the objective of tuning the parameters of a disturbance observer based torque control capable of compensating for the disturbances caused by the varying loads. It is shown that this method is capable of obtaining better performance than traditional H-infinity methods solving the overconservatism issue. The second considered method uses mu-synthesis to obtain a controller that achieves robust performance for a range of varying load inertias. The obtained controller, however, is not viable in a real system due to the large magnitude and frequency components of the control signal.

Contents

1 Introduction

In recent years, force control has seen a widespread adoption due to its usefulness in applications where the environment in which the robot will be operating is unknown, the robot will be operating with humans or animals and those in which collisions are expected [1, 2, 3]. Series elastic actuators (SEA) have been implemented in such applications due to some clear advantages over conventional stiff actuators. SEA are actuators in which a compliant element is deliberately introduced between the actuator and the load. This can benefit shock tolerance, energy storage and power output [2, 3]. At the same time, the force can be estimated by measuring the deflection of the compliant element [1].

A variety of force control algorithms have been used in combination with SEA. In many cases traditional PID-like structures are used [4]. Cascade PID controllers are also used in such applications [5]. More advanced methods such as H_2-optimal controllers [6] have been used.

Another control structure that is widely used is disturbance observer (DOB) based controllers. Such controllers usually contain a PID-like controller, an optional feedforward loop and an inner DOB loop. These controllers are popular because they can reject complex nonlinear dynamics without the need of modeling them [7].

In [8], a DOB based approach was developed. The controller parameters for the feedback loop and the inner DOB loop are found independently. A minimization function is used to find the optimal derivative gain for a given proportional gain. $\mathcal{H}_\infty$-optimization is used to find the DOB low-pass filter that ensures robust stability. The second step relays on the small gain theorem, a sufficient but not necessary condition to ensure robust stability [9]. This means that, in some cases, it is a restrictive constraint. The result obtained with the approach is more robust than necessary. This is an undesired consequence of the use of $\mathcal{H}_\infty$ and the small gain theorem called overconsrevatism. Decreasing overconservatism could improve the performance while maintaining the system sufficiently robust.

The aim of this project is to analyze the controller design and propose a new synthesis method with the objective of decreasing the overconservativism and, thus, increase the performance while maintaining the robustness. Two methods will be investigated. The first one consists in formulating the design approach as an optimization problem. The objective function and constraints have to be chosen such that a balance between performance and robustness is achieved. The second method consist in implementing μ-synthesis to obtain a controller that ensures robust stability and performance.

1.1 Contributions

The controller design is proposed as an optimization problem, something that was not found in literature in combination with series elastic actuators. This method allows to obtain robust performance increasing performance and reducing the overconsrevatism obtained with other commonly used methods.

The use of DOBs results in controllers that are robust to changes in load inertias without having to model their dynamic behaviour. This makes them ideal for use with articulated robots.

The optimization method makes the implementation of requirements in both the frequency and time domain easier to implement than other conventional methods.

1.2 Outline

In section 2, the background knowledge used in the project is explained, as well as the controller that will be used to compare the results. In section 3, the two different control design approaches will be discussed. The first one defines the controller design as an optimization problem. It is explained in a separate report that is supposed to be self-sustained. Because of this, some important information is repeated. The self-sustained report is the core of the project. The second approach uses μ-synthesis to obtain a robust controller. and is explained next. In section 4 contains a theoretical analysis of the obtained controllers. Section 5 briefly explains the results obtained in simulations performed with the help of the Compliant Joint Toolbox. Section 6 contains a discussion of the results.

2 Background

2.1 Series Elastic Actuators

Series-elastic actuators are actuators in which a spring is deliberately introduced between the actuator and the load [1]. Adding this compliant element can benefit shock tolerance, energy storage and power output while estimating the output force by measuring the deflection of the compliant element [1, 2, 3].

Figure 1 shows the ideal physical model of a SEA. There are three bodies: I_m represents the rotational inertia of the motor, I_g is the rotational inertia of the gears and I_l represents the load inertia. The two inputs of the system are the motor torque τ_m and the external torques τ_e. The deflection between the gear and the load is $\Delta = q_g - q_l$. The deflection is measured to estimate the output torque [8].

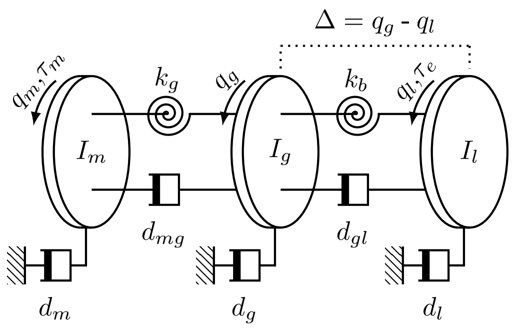

Figure 1: Ideal physical model of a series elastic actuator.

The equations of motion can be obtained from the torque balance of figure 1:

$$\begin{array}{rlll} I_m\ddot{q}_m = \tau_m & -d_m\dot{q}_m & + d_{mg}(\dot{q}_g - \dot{q}_m) & +k_g(q_g - q_m) \\ I_g\ddot{q}_g = & -d_g\dot{q}_g & - d_{mg}(\dot{q}_g - \dot{q}_m) & -k_g(q_g - q_m) \\ & & + d_{gl}(\dot{q}_l - \dot{q}_g) & +k_b(q_l - q_g) \\ I_l\ddot{q}_l = \tau_e & -d_l\dot{q}_l & - d_{gl}(\dot{q}_l - \dot{q}_g) & -k_g(q_k - q_g) \end{array} \tag{1}$$

The gear inertia can usually be neglected when compared to the load inertia, which is usually significantly larger, and to the motor inertia due to the increment of the apparent inertia caused by the gear ratio. Making I_g zero, performing the Laplace transform on the first two terms of equation 1 and rewriting the equations in terms of the deflection Δ, equation 2 is obtained [8].

$$\left[\alpha_1 s^3 + \alpha_2 s^2 + \alpha_3 s + \alpha_4\right] \Delta(s) = \alpha_5(s)\tau_m(s) - \alpha_6(s)q_l(s) \tag{2}$$

with,

$$\begin{aligned} \alpha_1 &= I_m\left(d_{mg} + d_{gl}\right) \\ \alpha_2 &= I_m\left(k_g + k_b\right) + d_{mg}\left(d_m + d_{gl}\right) + d_{gl}d_m \\ \alpha_3 &= k_g\left(d_m + d_{gl}\right) + k_b\left(d_{mg} + d_m\right) \\ \alpha_4 &= k_b k_g \\ \alpha_5\left(s\right) &= d_{mg}s + k_g \\ \alpha_6\left(s\right) &= I_m d_{mg}s^3 + \left(I_m k_g + d_m d_{mg}\right)s^2 + d_m k_g s \end{aligned} \tag{3}$$

The torque transmitted to the load is given by $\tau = k_b\Delta + d_{gl}\dot{\Delta}$ or, in the Laplace domain, by $\tau(s) = (k_b + d_{gl}s)\Delta(s)$. Using this knowledge and equation 2, the generated torque can be written as a function of τ_m and q_l[8]:

$$\tau(s) = (k_b + d_{gl}s)\left[\Delta_{\tau_m}(s)\tau_m(s) + \Delta_{q_l}(s)q_l(s)\right] \tag{4}$$

with,

$$\Delta_{\tau_m}(s) = \frac{\Delta(s)}{\tau_m} = \frac{\alpha_5(s)}{\alpha_1 s^3 + \alpha_2 s^2 + \alpha_3 s + \alpha_4} \tag{5}$$

$$\Delta_{q_l}(s) = \frac{\Delta(s)}{q_l} = \frac{-\alpha_6(s)}{\alpha_1 s^3 + \alpha_2 s^2 + \alpha_3 s + \alpha_4} \tag{6}$$

The obtained model can be written as shown in figure 2. The actuator dynamics are described in equation 4. If the path from τ to q_l is closed, the model including the load inertia is obtained. The nominal plant will be the actuator model shown in equation 7. The nominal open-loop plant from q_l is defined as $P_{q_l,n} = \Delta_{q_l}(s)(k_b + d_{gl}s)$. The disturbed plant can then be defined as shown in equation 8 with the load admittance given by $P_{load} = (I_l s^2 + d_l s)^{-1}$ [8].

$$P_n = \Delta_{\tau_m}(s)(k_b + d_{gl}s) \tag{7}$$

$$P = \frac{1}{I_l s^2 + d_l s} \tag{8}$$

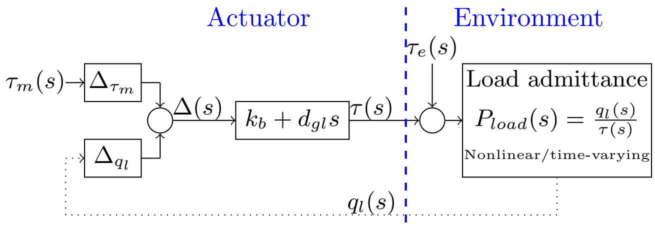

Figure 2: Torque dynamics of a SEA driving a load admittance $P_{load}(s)$ [8].

The SEA were modeled in MATLAB with the help of the Compliant Joint Toolbox is used[1]. This toolbox contains different models for series elastic actuator. In this case, the lumped gearbox model is used. This model has a negligible gearbox inertia. The toolbox can also be used to generate realistic SIMULINK model for validation purposes [10].

2.2 $\mathcal{H}_\infty$ design

Many control systems can be written in the general control configuration shown in figure 3. This system is described by using the equations 9 and 10. With u being the control parameters, v the measured variables, w the external inputs and z the error signals to be minimized [11].

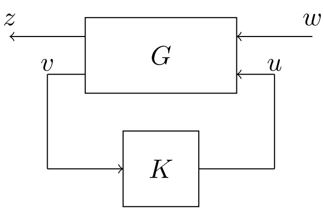

Figure 3: Synthesis framework.

$$\begin{bmatrix} z \\ v \end{bmatrix} = P(s) \begin{bmatrix} w \\ u \end{bmatrix} = \begin{bmatrix} P_{11}(s) & P_{12}(s) \\ P_{21}(s) & P_{22}(s) \end{bmatrix} \tag{9}$$

$$u = K(s)v \tag{10}$$

The transfer function from w to z is given by the linear fractional transformation in equations 11 and 12.

[1]Compliant Joint Toolbox on GitHub: `https://github.com/geez0x1/CompliantJointToolbox`

$$z = F_l(P, K)w \tag{11}$$
$$F_l(P, K) = P_{11} + P_{12}K(I - P_{22}K)^{-1}P_{21} \tag{12}$$

$\mathcal{H}_\infty$ control design consitst in finding the controller K that minimizes the $\mathcal{H}_\infty$-norm of the $F_l(P, K)$ function. There are different control algorithms that can be applied depending on the type of problem [11].

Mixed sensitivity $\mathcal{H}_\infty$ control

Mixed-sensitivity control problems are those in which the sensitivity function $S = (I + GK)^{-1}$ is shaped along with one or more other closed-loop transfer functions. The most commonly used transfer functions are the complementary sensitivity function $T = 1 - S$ and the transfer function from w to u (KS). A weight function is added to each of the transfer functions that allows to set requirements, knowledge of the frequency content of the input signals or relative importance of the functions. Stating the problem in this way allows to find a tradeoff between performance and robustness [11].

Signal-based $\mathcal{H}_\infty$ control

Signal based $\mathcal{H}_\infty$ control is an approach that covers a broad range of problems in which several objectives need to be met simultaneously. Using this approach, the plant can be defined with model uncertainties, the type of external disturbances is defined as well as the norm of the error signals to be minimized. [11]

Weights can be used to define the frequency content of the input signals as well as the desired frequency ranges of the error signals. Weights can also be used to model the uncertainties of the system according to the small gain theorem explained later on. All the weights need to be stable and proper to be able to apply the algorithm [11].

One example of such a problem is shown in figure 4. This control method tries to approximate the closed-loop response of the system to the ideal closed-loop response W_{model}. The weights W_{cmd}, W_{dist} and W_{snois} are used to specify the frequncy content of the input signals (d_{1-3}). The weights W_{act}, W_{perf1} and W_{perf} are used to specify the required frequency content of the error signals (e_{1-3}). The block H_{sens} contains the model of the sensors [12].

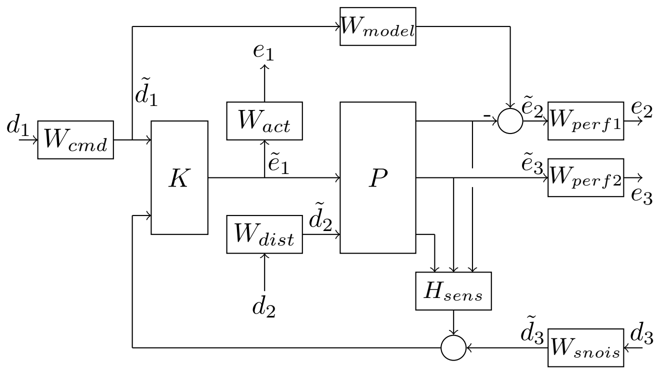

Figure 4: Generalized block diagram with weights used in H_∞ design [12].

Robust stability

The small gain condition

$$||H\Delta||_\infty \leq 1 \tag{13}$$

ensures robust stability. By the submultiplicative property of the $\mathcal{H}_\infty$ norm we have that $||H\Delta||_\infty < ||H||_\infty||\Delta||_\infty$ So, for equation 13 to hold, it is sufficient condition that

$$||H||_\infty||\Delta||_\infty < 1 \tag{14}$$

By definition, the norm of the uncertain part (Δ) is smaller than one. So, by minimizing the $\mathcal{H}_\infty$ norm of the interconnection matrix H over all stabilizing controllers K, the obtained controller will be optimally robust against perturbations Δ [9, 11].

Since this is a sufficient but not necessary condition, sometimes, the obtained controller is more robust than necessary. This also comes with a lower performance than what could be achieved [11].

2.3 $\mu-$ synthesis

Any interconnected system can be rearranged as shown in figure 5a, which is called the general framework. The controller can be absorbed into the interconnection structure to form the analysis framework shown in figure 5b. Any frequency domain linear time invariant (FDLTI) system with FDLTI disturbances can be written in the form of the generalized framework and, thus transformed into the analysis framework [13].

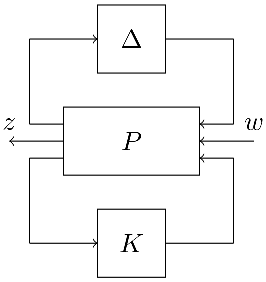

(a) Generalized framework

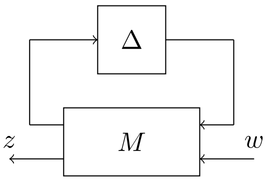

(b) Analysis framework

Figure 5: Generalized form of the system.

For a system written in the analysis framework, the structured singular value (SSV) is defined as an operator in definition 2.1.

Definition 2.1. *For $M \in C^{nxn}$, $\mu_{\boldsymbol{\Delta}}(M)$ is defined as*

$$\mu_{\boldsymbol{\Delta}} := \frac{1}{\min\{\bar{\sigma}(\Delta) : \Delta \in \boldsymbol{\Delta}, \det(I - M\Delta) = 0\}} \tag{15}$$

unless no $\Delta \in \boldsymbol{\Delta}$ makes $I - M\Delta$ singular, in which case $\mu_{\boldsymbol{\Delta}}(M) := 0$ [13].

The structured singular value gives the necessary and sufficient condition for robust stability. This is a better solution to other analysis methods since it does not have the overconservatism issue. A synthesis method that minimizes the μ-peak value will generate a robust controller that minimizes the overconservatism [11, 14].

D-K iteration algorithm

The μ-optimal controller,K can be found using the D-K iteration algorithm defined in [13] as follows:

(i) Fix an initial estimate of the scaling matrix $D_\omega \in \mathcal{D}$.

(ii) Find scalar transfer functions $d_i(s)$, $d_i^{-1}(s) \in \mathcal{RH}_\infty$ for $i = 1, 2, ..., (F-1)$ such that $|d_i(j\omega)| \approx d_i^\omega$.

(iii) Let

$$D(s) = diag(d_1(s)I, ..., d_{F-1}(s)I, I)$$

Construct a state space model for system

$$\hat{G}(s) = \begin{bmatrix} D(s) & \\ & I \end{bmatrix} G(s) \begin{bmatrix} D^{-1}(s) & \\ & I \end{bmatrix}$$

(iv) Solve an $\mathcal{H}_\infty$-optimization problem to minimize

$$||\mathcal{F}_l(\hat{G}, K)||_\infty$$

over all stabilizing K. Note that this optimization problem uses the scaled version of $\hat{G}$. Let its minimization controller be denoted by $\hat{K}$.

(v) Minimize $\bar{\sigma}[D_\omega \mathcal{F}_l(G, \hat{K}) D_\omega^{-1}]$ over D_ω, pointwise across frequency. Note that this evaluation uses the minimizing $\hat{K}$ from the last step, but that G is unscaled. The minimization itself produces a new scaling function. Let this new function be denoted by $\hat{D}_\omega$.

(vi) Compare $\hat{D}_\omega$ with the previous estimated D_ω. Stop if they are close, but, otherwise, replace D_ω with $\hat{D}_\omega$ and return to step (ii).

This algorithm is applied in the `musyn` function of the Compliant Toolbox in MATLAB. The μ-synthesis problems can also be defined depending on the way the interconection matrix is defined as mixed sensitivity or signal-based problems [12].

2.4 DOB based SEA controller

In a previous project, a method for designing controllers for series elastic actuators was developed. The controller's structure is shown in figure 6. A PD controller and feedforward signal are used to achieve performance. The derivative control is applied to the output signal to avoid derivative kick. A disturbance observer is applied in the open loop configuration to eliminate the nonlinear disturbances caused by the varying load inertia.

$$
\begin{aligned}
C_1 &= K_p \\
C_2 &= K_d s \\
D_1 &= Q \\
D_2 &= Q P_n^{-1} \\
\lambda &= \frac{1}{||P_n(s=0)||}
\end{aligned}
\tag{16}
$$

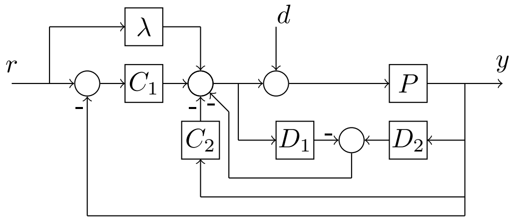

Figure 6: General structure of a disturbance observer DOB.

A method to find the optimal parameters for the PD control and DOB independently was developed. Root locus is used to find the appropriate derivative gain for a given proportional controller that achieves the desired relative damping. For this method, the loop gain has to be rewritten to be a function of the derivative action, as shown in equation 17, with the parameters of equation 3. The root locus can then be used to achieve the required level of damping for the controlled closed-loop nominal plant. Figure 7 shows the root-locus used to find the appropiate derivative gain for a proportional gain of 3. To achieve a relative damping of 0.875, a derivative gain of 0.019 would have to be used [8].

$$
L = \frac{\alpha_5 k_b s}{\alpha_1 s^3 + \alpha_2 s^2 + \alpha_3 s + \alpha_4 + \alpha_5(s) K_p k_b} \tag{17}
$$

This controller is developed for the nominal plant, however, the varying load inertia makes the system nonlinear and, thus, the controller will not perform as expected. The DOB is used to make the system behave as the nominal system independently of those nonlinearities and other possible system uncertainties or disturbances. $\mathcal{H}_\infty$ optimization was used to find the optimal low-pass filter to be used. The optimization technique uses the sensitivity and complementary sensitivity functions of the DOB loop, shown in equation 18. The weights in equation 19 are used to account for the inertia uncertainty (W_T) and to ensure some level of performance (W_S). The final interconnection matrix is shown in equation 20. Two different types of low-pass filters were used with this optimization technique (binomial and butterworth) with different orders. It was found that the 2nd order butterworth filter gave better results. The optimal cut-off frequency was 105.4 rad/s[8].

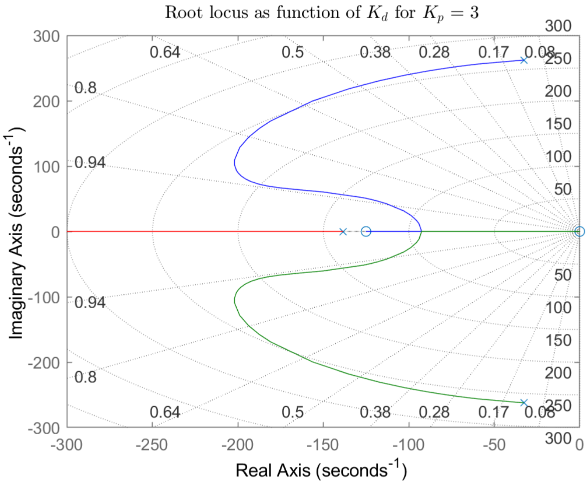

Figure 7: Root locus as a function of K_d

$$
\begin{aligned}
T &= Q \\
S &= (1 - Q)
\end{aligned}
\tag{18}
$$

$$
\begin{aligned}
W_T &= \frac{47.37s^2}{(a + 1885)(s + 251.3)} \\
W_S &= \frac{w_s^2}{s^2 + 2\zeta w_s s + w_s^2} \\
w_s &= 2\pi \cdot 15 \\
\zeta &= \frac{1}{\sqrt{2}}
\end{aligned}
\tag{19}
$$

$$
H_0 = \begin{bmatrix} W_T T & 0 \\ 0 & W_S S \end{bmatrix}
\tag{20}
$$

Some different performance metrics are used to analize the performance of the controller with and without DOB in the following figures. The black-dashed line represents the behaviour of the nominal system. The nominal system will behave equally whether the DOB is activated or not. The colored-continuous lines represent the controllers with a DOB and the colored-dashed lines represent the controller without the DOB. Each color represents a different load inertia. The different load inertias are logarithmically separated between 0.04 and 10. The arrow represents the direction of increasing inertias. Figure 8 shows the reference tracking with and without DOB for different load inertias as well as for the nominal case. The benefits in reference tracking caused by the DOB can be clearly seen. At higher frequencies however, the DOB becomes transparent and it approaches the case without DOB.

Figure 9 shows the disturbance rejection properties of the controller with and without DOB. It is shown that at lower frequencies, where the DOB acts, the disturbance rejection is increased dramatically. At higher frequencies it approaches the controller without DOB.

Figure 10 shows the noise rejection transfer function with and without DOB. It is shown that at lower frequencies the noise rejection deteriorates. This is because the measurement noise is seen as a disturbance by the DOB and compensated for. As before, at higher frequencies, the DOB does not act anymore and the signal approaches the one without DOB.

Figure 11 shows the nysquist plot of the system with DOB for different load inertias. It can be observed that the system is robustly stable for all load inertias. The system has infinite gain margin for all inertias and phase margin always above 75 degrees. These plots show clear advantages on using disturbance observers. For that reason, this structure will be used for the optimization.

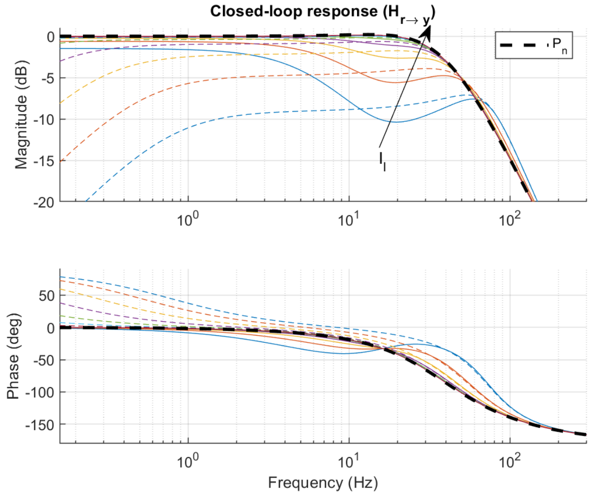

Figure 8: Reference tracking with DOB (continuous) and without DOB (dashed) compared to the nominal plant.

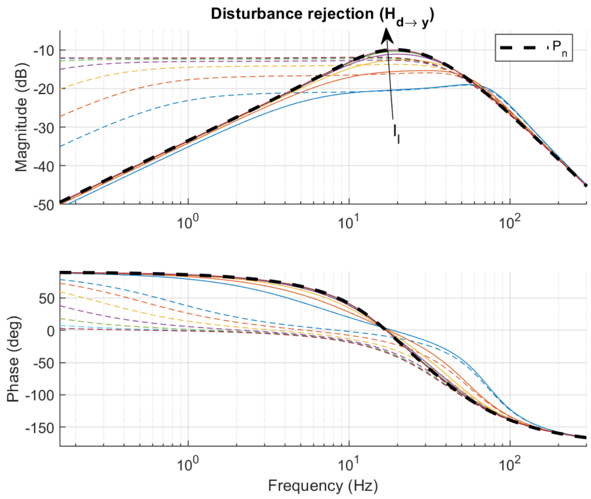

Figure 9: Disturbance rejection with DOB (continuous) and without DOB (dashed) compared to the nominal plant.

3 Approach

3.1 Optimization Problem

In this section, the controller design is defined as an optimization problem. This approach is the core of the report. The proposed method is explained in what is supposed to ba a self-sustained report. Because of this, some of the basic information may be repeated.

Relaxing Conservatism of Robust Disturbance Observer based Torque Control of Series-Elastic Actuators for Articulated Robots: An Optimization Problem

Luuk Lomillos Rozeboom
Robotics and Mechatronics
University of Twente
Enschede, The Netherlands
l.lomillosrozeboom@gmail.com

***Abstract*—The use of series elastic actuators for torque control of articulated robots has seen an increase in adoption in the last years due to some clear benefits with respect to conventional actuators. The dynamic behaviour of articulated robots is highly nonlinear. This paper focuses on the tuning of a disturbance observer based torque control capable of compensating for the disturbances caused by the varying loads. The proposed method defines the controller design as an optimization problem. It is shown that this method is capable of obtaining better performance than traditional H-infinity methods solving the overconservatism issue.**

I. Introduction

In recent years, force control has seen a widespread adoption due to it's usefulness in applications where the environment in which the robot will be operating is unknown, the robot will be operating with humans or animals and those in which collisions are expected [1, 2, 3]. Series elastic actuators (SEA) have been implemented in such applications due to some clear advantages over conventional stiff actuators. SEA are actuators in which a compliant element is deliberately added between the actuator and the load. This can benefit shock tolerance, energy storage and power output [2, 3]. At the same time, the force can be estimated by measuring the deflection of the compliant element [1].

A variety of force control algorithms have been used in combination with SEA. In many cases traditional PID-like structures are used [4]. Cascade PID controllers are also used in such applications [5]. More advanced methods such as H_2-optimal controllers [6] have been used. Another control structure that is widely used is disturbance observer (DOB) based controllers. Such controllers usually contain a PID-like controller, an optional feedforward signal and an inner DOB loop. These controllers are popular because they can reject complex nonlinear dynamics without the need of modeling them [7].

In a previous project, [8][1], a DOB based approach was developed. The controller parameters for the feedback loop and the inner DOB loop are found independently. Pole placement is used to find the optimal derivative gain for a given proportional gain. $\mathcal{H}_\infty$-optimization is used to find the DOB low-pass filter that ensures robust stability. The second step uses the small gain theorem, a sufficient but not necessary condition to ensure robust stability [9]. This means that, in some cases, it is a restrictive constraint. The result obtained with the approach is more robust than necessary. This is an undesired consequence of the use of $\mathcal{H}_\infty$ and the small gain theorem called overconservatism. Decreasing the overconservatism could improve the performance while maintaining the system sufficiently robust.

The aim of this project is to analyze the controller design and propose a new synthesis method with the objective of decreasing the overconservativism and, thus, increase the performance while maintaining the robustness. The proposed method consists in formulating the design approach as an optimization problem. The weight function and constraints have to be chosen such that a balance between performance and robustness is achieved.

This paper will start with a brief explanation of the important background. In section II a model for SEAs will be briefly explained, then the basic structure of a DOB, used to obtain robust performance will be introduced and, finally, the controller that was the starting point of the project, whose structure will be used will be shown. Section III will give a short explanation of the apprach that was followed. Section IV will contain the specifics of the implementation in MATLAB. In section V a analysis of the theoretical performance of the system will be discussed. Finally, section VI will discuss the results obtained in a simulation.

[1]This paper has not been published.

II. BACKGROUND

A. Series Elastic Actuators

Series-elastic actuators are actuators in which a spring is deliberately introduced between the actuator and the load [1]. Adding this elastic element can benefit shock tolerance, energy storage and power output. The output torque can be estimated by measuring the deflection of the compliant element, making the force measurement easy and accurate [1, 2, 3].

A series elastic actuator (SEA) can be represented with the diagram shown in Figure 1. The input of the system is the torque supplied by the motor (τ_m) and the output of the system is the torque applied to the load (τ). The dimension of the gear inertia is quite small compared to that of the motor. The differece in dimension is increased when the gear ratio is taken into account. To simplify the model, the gear inertia will be neglected. The dynamic equations of the model are derived in [8] and can be expressed in the frequency domain as follows:

$$\left[\alpha_1 s^3 + \alpha_2 s^2 + \alpha_3 s + \alpha_4\right] \Delta\left(s\right) = \alpha_5\left(s\right)\tau_m\left(s\right) - \alpha_6\left(s\right) q_l\left(s\right) \tag{1}$$

with,

$$\begin{aligned} \alpha_1 &= I_m\left(d_{mg} + d_{gl}\right) \\ \alpha_2 &= I_m\left(k_g + k_b\right) + d_{mg}\left(d_m + d_{gl}\right) + d_{gl} d_m \\ \alpha_3 &= k_g\left(d_m + d_{gl}\right) + k_b\left(d_m g + d_m\right) \\ \alpha_4 &= k_b k_g \\ \alpha_5\left(s\right) &= d_{mg} s + k_g \\ \alpha_6\left(s\right) &= I_m d_{mg} s^3 + \left(I_m k_g + d_m d_{mg}\right) s^2 + d_m k_g s \end{aligned} \tag{2}$$

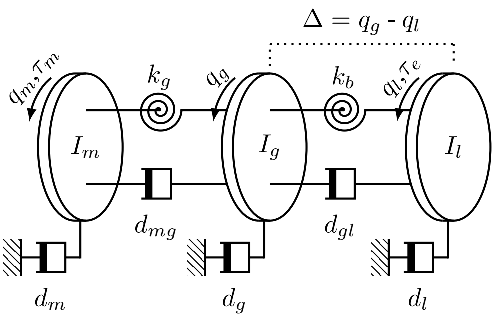

Fig. 1. Ideal physical model of a series elastic actuator.

The torque transmitted to the load can be written in terms of the deflection: $\tau = k_b\Delta + d_{gl}\dot{\Delta}$. For estimating the torque, the damping term d_{gl} is usually ignored and $\tau \approx k_b\Delta$ is used. Using the equation for the transmitted torque in the frequency domain, $\tau = (k_b + d_{gl}s)\Delta(s)$, and equation 1, the generated torque can be written as the sum of the inputs τ_m and q_l:

$$\tau(s) = (k_b + d_{gl}s)\left[\Delta_{\tau_m}(s)\tau_m(s) + \Delta_{q_l}(s)q_l(s)\right] \tag{3}$$

where

$$\begin{aligned} \Delta_{\tau_m}(s) &= \frac{\Delta(s)}{\tau_m(s)} = \frac{\alpha_5(s)}{\alpha_1 s^3 + \alpha_2 s^2 + \alpha_3 s + \alpha 4} \\ \Delta_{q_l}(s) &= \frac{\Delta(s)}{q_l(s)} = \frac{\alpha_6(s)}{\alpha_1 s^3 + \alpha_2 s^2 + \alpha_3 s + \alpha 4} \end{aligned} \tag{4}$$

This structure is shown in figure 2 as a block diagram. With an articulated robot, the load is a nonlinear dynamic model. In the analysis of this project it will be assumed that this model can be simplified as a frictionless point mass. So, the load model will be $\mathrm{P_{load}} = \mathrm{I_l^{-1}s^{-2}}$.

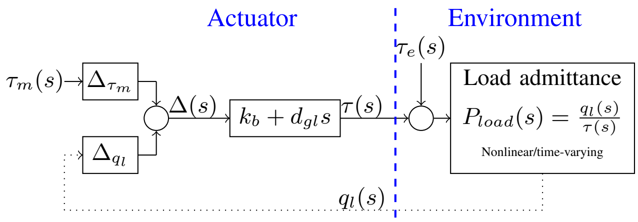

Fig. 2. Torque dynamics of a SEA driving a load admittance $P_{load}(s)$ [8].

B. Disturbance observers

Disturbance observers are a control structure used to estimate disturbances or uncertainties in the system. The basic structure of a DOB is shown in figure 3. The input of the plant is compared to the expected input calculated using the plant's output and the inverse of the nominal plant. This difference gives an estimate of the external disturbances, errors in the nominal plant and unmodeled dynamics. The estimated disturbance can then be fed back to compensate for it. In practice, this cannot be done because the inverse of the plant is nonproper. To compensate for this, a low-pass filter (Q) is added that has, at least, the same order as the plant [10].

There are two main limitations to DOBs. The first one is that, due to the low-pass filter, the DOB can only reject disturbances up to the cut-off frequency. However, in many cases, the required bandwidth is relatively low so, the cut-off frequency can usually be set high enough. The second one is the fact that the noise rejection decreases. This is because the DOB cannot differentiate between noise and the measure output so, it will consider the measurement noise to be a disturbance to be compensated. This last limitation decreases the robustness of the system [10].

DOBs have been used in torque controllers of SEAs for their ability to compensate for complex dynamic uncertainties without the need to model them. On top of that, DOBs do not affect the closed-loop frequency content of the nominal response. It works specially well removing steady-state error [7, 11].

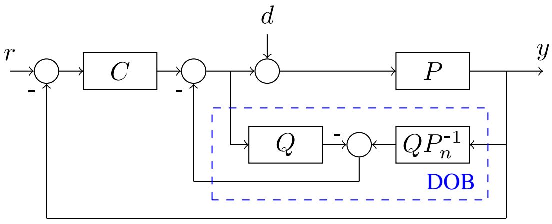

Fig. 3. General structure of a disturbance observer DOB.

C. Controller structure

To control the system, a proportional and derivative (PD) controller is used in order to achieve the required level of performance. In [8] a method to control the nominal plant of a SEA with a desired relative damping was developed. The method uses root locus to select the required damping parameter given a proportional parameter to achieve the specified damping ratio.

The disturbance observer is tuned using $\mathcal{H}_\infty$ optimization. The optimization is stated as a mixed sensitivity problem of the DOB's loop [9]. The problem with this approach is that, since the small gain theorem used with $\mathcal{H}_\infty$ optimiation to ensure robustness is a necessary but not sufficient condition, the resultant controller can be overconservative [12].

Figure 4 shows the block diagram of the closed-loop system. The plant shown in figure 2 is used. The system inside the purple block represents the nominal plant. When the blue-dashed loop is closed, the perturbated plant is obtained. The block P_l represents the load model. The red box of figure 4 shows the feedforward controller, which is obtained by evaluating the gain of the nominal reference tracking function ($H^n_{r\to y}$) evaluated at zero frequency. The orange box shows the PD controller, used to achieve performance. The green box shows the DOB. The function Q of the DOB is a low-pass filter. In this case a second degree butterworth filter was used. The different control blocks are shown in the following equation:

$$\begin{aligned} \lambda &= \frac{1}{\left|H^n_{r\to y}(s=0)\right|_2} \\ C_P &= K_p \ , \quad C_D = K_d s \\ D_1 &= Q \ , \quad D_2 = QP_n^{-1} \\ P_n &= \Delta_{\tau_m}(k_g + d_{gl}s) \end{aligned} \tag{5}$$

Figure 4 has one output and four inputs. The output y is the torque exerted on the load inertia [Nm]. The input r represents the torque that wants to be achieved at the output [Nm], d represents the disturbances applied on the input of the system [Nm], τ_e represents the external disturbances applied on the load [Nm] and n represents the measurement noise [Nm]. There are some other internal signals that could be of importance: e represents the error of the output signal, u is the control signal [Nm], the output of the controller, $\hat{d}$ is the estimated disturbance and q_l is the position of the load [m].

There are several functions that can be useful for the analysis of the system's performance:

1) $\mathrm{H_{r\to y}}$ is the reference tracking. It represents the relation between the desired and obtained output. It can be calculated with the expression:

$$H_{r\to y} = \frac{C_p + \lambda P}{1 + \delta Q + PC} \tag{6}$$

2) $\mathrm{H_{d\to y}}$ is the disturbance rejection. It represents how much a disturbance affects the output.

$$H_{d\to y} = \frac{(1-Q)P}{1 + \delta Q + PC} \tag{7}$$

3) $\mathrm{H_{n\to y}}$ is the noise rejection. It represents how much the measurement noise is transmitted to the output.

$$H_{n\to y} = \frac{-(1+\delta)(CP_n + Q)}{1 + \delta Q + PC} \tag{8}$$

4) $\mathrm{H_{q_l\to y}}$ is the transparency. It represents how much torque is generated by the load motion.

$$H_{q_l\to y} = \frac{(1-Q)P_{q_l}}{1 + \delta Q + PC} \tag{9}$$

5) $\mathrm{H_{r\to u}}$ represents the work done by the controller to follow a given reference

$$H_{r\to u} = \frac{\lambda + C_p}{1 + D_1} \tag{10}$$

III. Approach

The goal is to obtain a controller design that maximizes performance while remaining sufficiently robust. To achieve that, the objective will be stated as a minimization function. The general for of such a problem is stated in the following equation:

$$\begin{aligned} \min \quad & f(\mathbf{x}) \\ \text{s. t.} \quad & \underline{\mathbf{x}} \le \mathbf{x} \le \overline{\mathbf{x}} \\ & \mathbf{g}(\mathbf{x}) \le \mathbf{0} \\ & \mathbf{h}(\mathbf{x}) = \mathbf{0} \end{aligned} \tag{11}$$

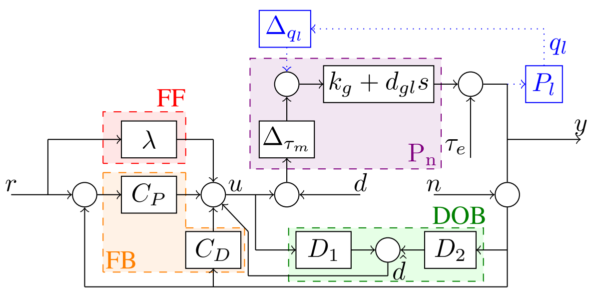

Fig. 4. Block diagram of the controlled system.

The variable $\mathbf{x} \in \mathbb{R}^n$ is called the optimization variable. The function $f : \mathbb{R}^n \rightarrow \mathbb{R}$ is called the objective function and is what will be minimizad. The variables $\underline{x}_i$ and $\overline{x}_i$ are the lower and upper bounds respectively of each optimization variable x_i. The functions $g_j : \mathbb{R}^n \rightarrow \mathbb{R}$ are called the inequality constraint functions, collected in the vector $\mathbf{g}$, and the functions $h_k : \mathbb{R}^n \rightarrow \mathbb{R}$ are the equality constraint functions, collected in the vector $\mathbf{h}$ [13].

The controller structure used is the same as the one shown in figure 4. There are three variables of the system: the proportional and derivative actions (K_p and K_d) of the controller and the cut-off frequency (ω_c) of the DOB. In [8], a method to find the derivative gain that achieves a relative damping given a proportional gain is proposed. Using this reduces the problem to two dimensions while ensuring that the desired damping is achieved. However, two minimization will have to be performed sequentially, making the problem computationally expensive. To avoid this, the appropriate derivative action can be found for the range of proportional gains that are considered in the minimization and, then, a polynomial can be fit to the data. This is shown in figure 5, where the black line shows the ideal derivative gains for a specific proportional gain and the red line is a fitted 8^{th} degree polynomial. Using this polynomial will make the minimization more efficient. Using this approach, the optimization variables become $\mathbf{x} = [K_p, \omega_c]$.

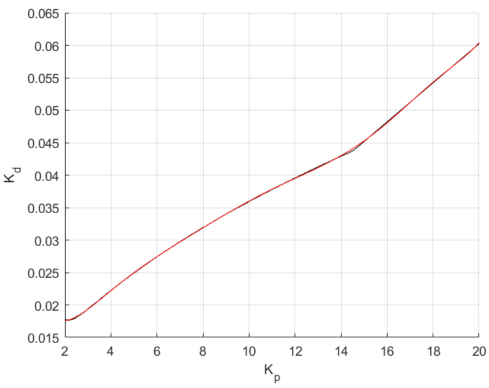

Fig. 5. Needed derivative gain to obtain a 0.875 closed-loop relative damping of the nominal plant for a given proportional gain.

The objective function is used to maximize performance. Different metrics could be used to construct this function [12]. It may be that one metric is not enough to ensure performance and more than one function needs to be minimized. In such cases, the different functions can be added as shown in equation 12. The vector $\mathbf{f}(\mathbf{x})$ contains the subfunctions that need to be combined. The vector $\mathbf{w}$ contains different weight functions that can be used to determine the relative importance of the different subfunctions. Finally, the result of the scalar product of these two vectors can be devided by the sum of the weight vector elements to normalize the function.

$$f(\mathbf{x}) = \frac{\mathbf{w} \cdot \mathbf{f}(\mathbf{x})}{\sum_{i=1}^{N} \mathrm{w}_i} \tag{12}$$

The controller should maximize performance while staying sufficiently robust. The metric used to define performance is the closed-loop bandwidth. However, bandwidth has to be maximized so, to be implemented in the minimization, the inverse of the bandwidth is used.

Adding a weight function that increases the work done by the DOB can improve the robustness of the system. Different functions can be considered to achieve this. In most cases, the disturbance rejection can be used. However, in the cases where information about the disturbance are known, that should be added into the system. In this specific example, the main expected disturbance is the one caused by the load. The transfer function from q_l to y shows the effect on the output from a displacement of the load. This is not exactly the dynamic behavior caused by the load. However, it includes only the disturbances caused by the load. The shape of this transfer function is shown in figure 6. It is shown that at lower frequencies the DOB ensures that the effect of q_l is negligible. However, at higher frequencies, the response tends to a constant value. At those higher frequencies, the magnitude of the frequency response is that of the compliance between the actuator and the load. Another interesting property of this function is that it can be rewritten as a weighted disturbance of the nominal plant as shown in equation 13.

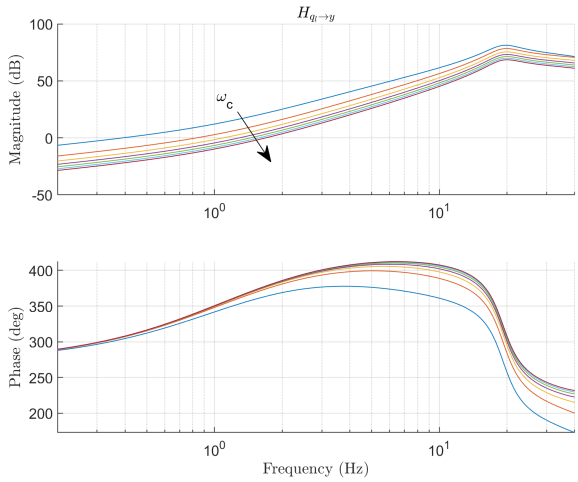

Fig. 6. Frequency response of the transparency transfer functions ($H_{q_l \rightarrow y}$) with different DOB low-pass cut-off frequencies. The increasing cut-off frequencies are in the direction of the arrow.

$$H_{q_l \rightarrow y} = \frac{\Delta_{\tau_m}}{\Delta_{q_l}} H^n_{d \rightarrow y} \tag{13}$$

This information is added to the objective function is by using the 0 dB crossover frequency. It can be clearly seen that, the higher the crossover frequency, the larger the rejection of the load disturbance. For this reason, the inverse of the 0 dB crossover frequency can be used as a weight function.

These two functions can be implemented into the objective function using equation 12. If the vector $\mathbf{w}$ is defined as $[w, 1-w]$, equation 14 is obtained.

$$f_0 = w \cdot \frac{1}{\omega_{-3dB}\left(H_{r\to y}\right)} + (1-w)\,\frac{1}{\omega_{0dB}\left(H_{q_l\to y}\right)} \tag{14}$$

The lower and upper bounds, $\underline{\mathbf{x}}$ and $\overline{\mathbf{x}}$ respectively, are used to ensure that the algorithm will not apply positive feedback. In the cases where the optimiazation variable is a cut-off frequency, the boundaries are used to ensure that the variable is both positive and below the nyquist frequency.

Requirements can usually be set as an inequality constraint: there is an acceptable value for a performance metric, however, it would be ideal to be either below or above that value. For the minimization to be valid, the system should satisfy all the inequality constraints.

To ensure robustness, the phase, gain and delay margins were considered [12]. The gain margin was found to be infinite for all the control parameters in the considered range so, it was left out to improve the speed of the algorithm. The phase margin was set to have a minimum of $\underline{PM}$ and the delay margin to have a minimum of $\underline{DM}$. Besides that, the $\mathcal{H}_\infty$ norm of the controller work transfer function, $H_{r\to u}$, was set to have a maximum gain of $\overline{u}$. This function will ensure that the control signals can be reproduced by the actuator of the real system. Finally, a minimum closed-loop bandwidth of $\underline{\omega}$ is required. Equation 15 shows the inequality constraint functions.

$$f = -\begin{bmatrix} PM(\omega_c, K_p) - \underline{PM} \\ DM(\omega_c, K_p) - \underline{DM} \\ \omega_{-3dB}(H_{r\to y}) - \underline{\omega} \\ |H_{r\to u}|_\infty - \overline{u} \end{bmatrix} \leq \mathbf{0} \tag{15}$$

Choosing the initial conditions for the minimization algorithm is important to ensure the absolute minimum is found. A propose approach to find the initial values of the minimization is shown in algorithm 1. A number of equally spaced values of optimization variables are set between the minimum and maximum boundary values. The optimization function is then evaluated for all the possible combinations using nested for-loops. Finally, the objective function is evaluated at all the optimization values for which the equality and inequality constraints hold. And the values of the optimization variable that achieve the minimum objective function's value will be the initial value for the minimization algorithm. This method does not ensure that the absolute minimum will be found, however, in most cases, it will increase the chances of finding it.

Algorithm 1: Finding the initial values for the minimization algorithm.

choose N_1 to N_n; `// high values will take long but get closer to the abs. min.`
x_1 = [N_1 values linearly spaced from l_1 to u_1];
x_2 = [N_2 values linearly spaced from l_2 to u_1];
$\vdots$
x_n = [N_n values linearly spaced from l_n to u_n];
for i_1 = *1:*N_1 **do**
  for i_2 = *1:*N_2 **do**
    $\vdots$
    for i_n = *1:*N_n **do**
      `// Evaluate the constraints`
      $f_v(i) = f(x(i))$;
      $g_v(i) = \prod_{k=1}^{N_k} \left(g_k(x(i)) \leq 0\right)$;
      $h_v(i) = \prod_{k=1}^{N_k} \left(h_k(x(i)) = 0\right)$;
      `// If constraints do not hold`
      if $\neg(g_v(i) \wedge h_v(i))$ **then**
        $\mathrm{f_v}(i)$ = NaN; `// Ignore`
      end
    end
  end
end
find i s.t $f_v(i) = \min(f_v)$;
x_0 = $[x(i)]$;
or
find $i_1, i_2, \ldots, i_n$ s.t $f_v(i_1, i_2, \ldots, i_n) = \min(f_v)$;
x_0 = $[x_1(i_1), x_2(i_2), \ldots, x_n(i_n)]$;

IV. Implementation

In this section, the proposed approach is implemented in MATLAB to demonstrate how the weight functions and constraint equations could be selected. The controller obtained with the proposed method will be compared with the one shown in [8]. For this reason, the same SEA model and parameters will be used. The SEA will be modelled with the help of the Compliant Joint Toolbox for MATLAB. The parameters used for the model are shown in table I and are the same as those used in reference [8]. The load inertia has a range between 0.04 and 10 $\mathrm{kg\,m^2}$. From analysis of the different metrics used in the optimization it was found that the lowest inertia gave the worst performance and robustness. To ensure that the results will be equal or better than the set requirements for all the range of inertias the lowest inertia of 0.04 $\mathrm{kg\,m^2}$ was used for the optimization.

As stated before, the optimization variables will be $\mathbf{x} = [K_p, \omega_c]$. The lower limit will be used to ensure that both variables will be larger than 0: $\underline{\mathbf{x}} = [0, 0]$. The upper limit

Parameter		Value	
Gearbox ratio	n	80	
Torque constant	k_τ	0.078	[N m A^{-1}]
Rotor+gear inertia	I_m	0.295	[kg m^2]
Rotor+gear viscous	d_m	2.22	[N m s rad^{-1}]
Load viscous friction	d_l	0	[N m s rad^{-1}]
Rotor+gear Coulomb	$d_{c,m}$	3.54	[N m]
Load Coulomb friction	$d_{c,l}$	0	[N m]
Gear internal viscous	d_{mg}	80	[N m s rad^{-1}]
Sensor internal viscous	d_{gl}	0	[N m s rad^{-1}]
Gearbox stiffness	k_g	10^4	[N m rad^{-1}]
Sensor stiffness	k_b	5714	[N m rad^{-1}]

TABLE I
PARAMETERS USED FOR THE SEA MODEL [8].

will be somewhat arbitrary, ensuring that the proportional gain is below 20 and the cut-off frequency is not above 1500 rad/s: $\overline{\mathbf{x}} = [20, 1500]$.

The phase margin is chosen to be $\underline{PM} = 45deg$, the delay margin was chosen to be $\underline{DM} = 1.25ms$, the minimum bandwith to be $\underline{\omega} = 40rads^{-1}$ and the maximum controller gain to be $\overline{u} = 15dB$

Once all the functions are defined, the minimization algorithm can be run. It is run for 10 different values of K_p and ω_c between and including the boundary constraints. Using the obtained initial conditions, the minimization algorithm is run and the optimal values are found to be $\omega_c = 596.34$ and $K_p = 10.25$, with a corresponding $K_d = 0.0365$.

Figure 7 shows the results of the minimization algorithm with the specified functions. The boundaries of the constraints are the different colored lines. The colored area represents the combination of proportional gains and cut-off frequencies that would produce a controller that meets the requirements. The yellow colors represent the higher values of the objective function and the blue colors the lower values. The green cross shows the initial conditions of the minimization function and the red star is the optimal controller found by the minimization algorithm. It was found that the optimal controller will always be in the boundary of the strictest inequality constraints, and, in many cases, in the intersection between two constraints.

V. ANALYSIS

As stated before, a case study is used to demonstrate the viability of the design method. The functions used in the minimization are explained in section III. The used settings are explained in section IV. After running the minimization algorithm a controller is obtained. This controller has the structure of figure 3 with the parameters: $K_p = 10.25$, $K_d = 0.0365$ and $\omega_c = 596.34$.

The performance of the controller is analyzed using different transfer functions. The results are compared with the controller obtained in [8], where $\mathcal{H}_\infty$ was used to obtain a robust controller that was slightly overconservative, with the parameters: $K_p = 3$, $K_d = 0.019$ and $\omega_c = 105.4$. The first

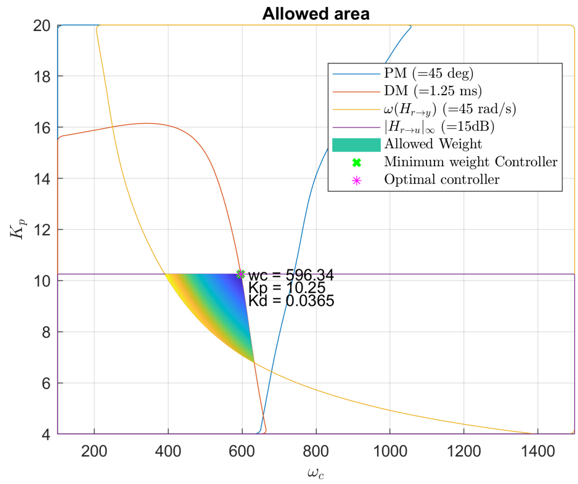

Fig. 7. Objective function, boundary of the constraints and initial and final points of the minimization algorithm.

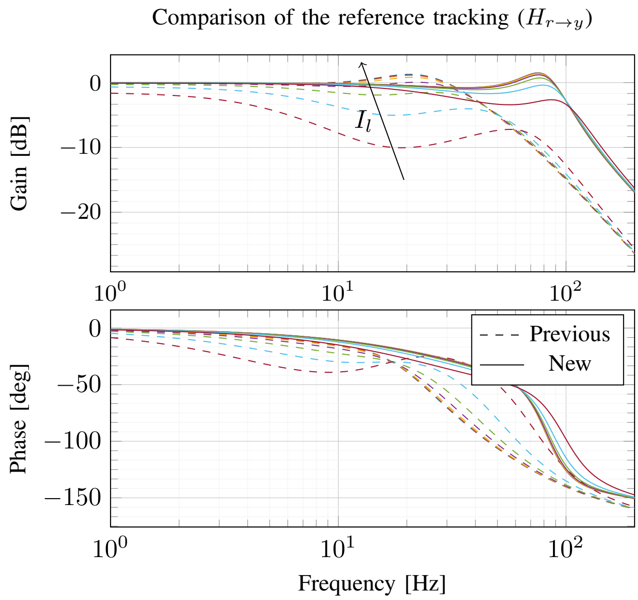

Fig. 8. Comparison of the reference trakcing obtained with the method proposed in [8] (Previous) with the one obtained with the method proposed (New)

transfer function to be analyzed is the reference tracking. The bode plot is shown in figure 8. The solid lines represent the controller obtained in this report, whereas the dashed lines represent the previous controller tuned using $\mathcal{H}_\infty$ synthesis. This distinction will used in all the plots of this section. It is shown that the obtained controller has a larger bandwidth and the closed loop response is more consistent for the entire range of load inertias.

The next two metrics are related to the robustness of the system to unwanted inputs. The first one is the disturbance rejection, which is shown in figure 9. It is shown that the disturbance rejection is significantly larger. Figure 10 shows the noise rejection. At lower frequencies it is similar than for the comparison controller, however, for higher frequencies it is slightly worse. This is one of the limitations of DOBs: the measurement noise is treated as a disturbance and compensated for, this causes it to appear in the output of the plant. This limitation is accentuated in the new controller since the DOB's cut off frequency has been increased.

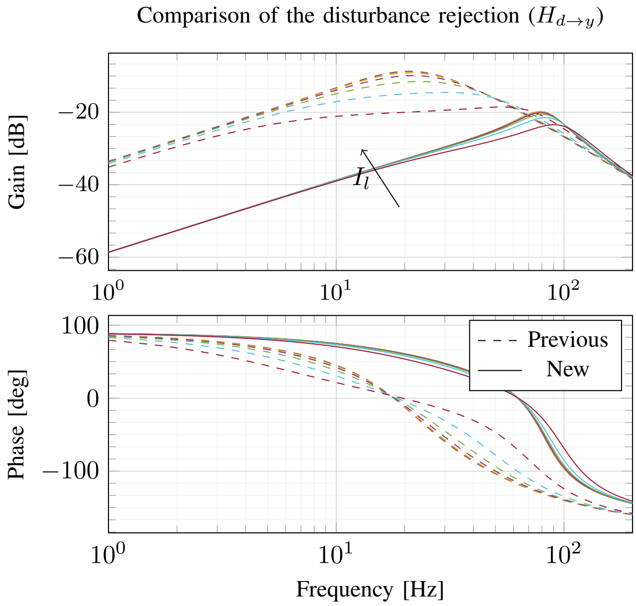

Fig. 9. Comparison of the disturbance rejection obtained with the method proposed in [8] (Previous) with the one obtained with the method proposed (New)

Figure 11 shows the Nyquist plot of the system. It is shown that the controller is stable for all the range of load inertias. A phase margin of 55 deg is obtained. The delay margin is 1.25, which is the minimum allowable margin. The gain margin remains infinite as was observed to be for all the considered parameters.

VI. Simulation

The simulation is done in Simulink with the help of the Compliant Joint Toolbox. This toolbox contains models of different types of SEAs. This models also contains the addition of measure noise and other disturbances. The model is used to replace the plant of figure 3. The controller is implemented as shown in the figure.

The input reference signal is a frequency sweep signal between 0.1 and 200 Hz in a time span of 200 seconds. The amplitud of the reference signal goes from 10 to -10 Nm^2.

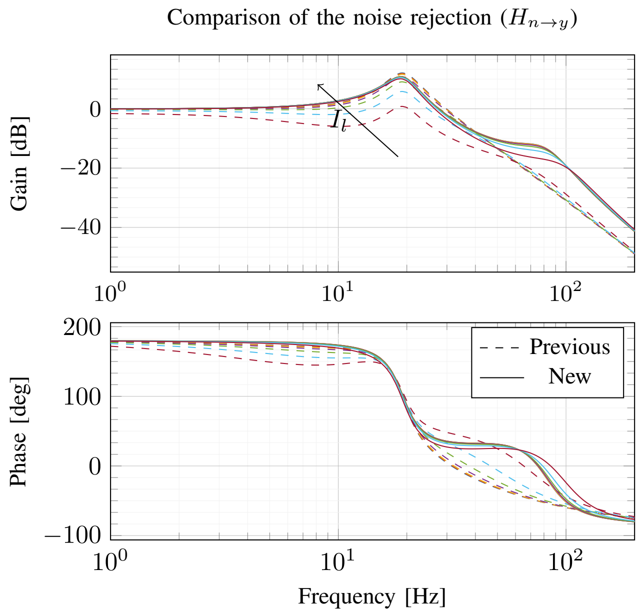

Fig. 10. Comparison of the noise rejection obtained with the method proposed in [8] (Previous) with the one obtained with the method proposed (New)

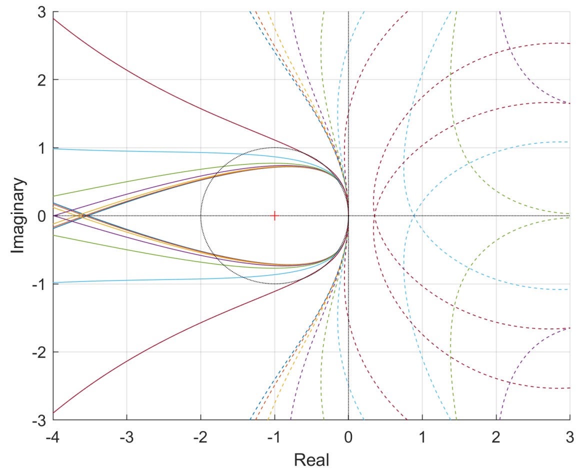

Fig. 11. Nyquist plot of the obtained controller with the optimization method.

For the disturbances, input noise with a variance of 0.021 and a measurement noise with a variance of 1e-10 is added to the SEA model. The load inertia of the SEA was set to 0.04 $\mathrm{kg\,m}^2$, which is the inertia that represent the largest disturbance and, thus, should give the worst results.

A. *Discretization*

To implement the controller in a real system, it has to be discretized first. The continuous and discrete functions are evaluated at different frequencies and the error and standard deviation of the different methods can then be calculated. Figure 12 shows the continuous controller compared with the discretized ones. Figure 13 shows the error and standard deviation of the different discretized controllers. The least-squares method seems to be the one that matches the controller more accurately.

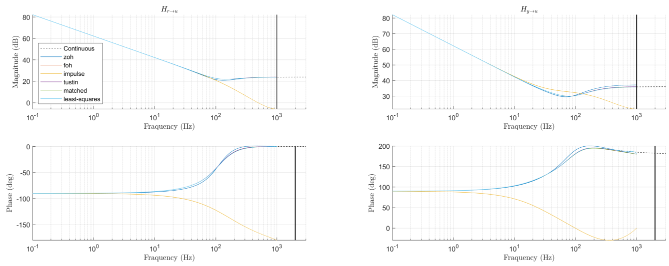

Fig. 12. Continuous controller compared with the discretized controller using different methods.

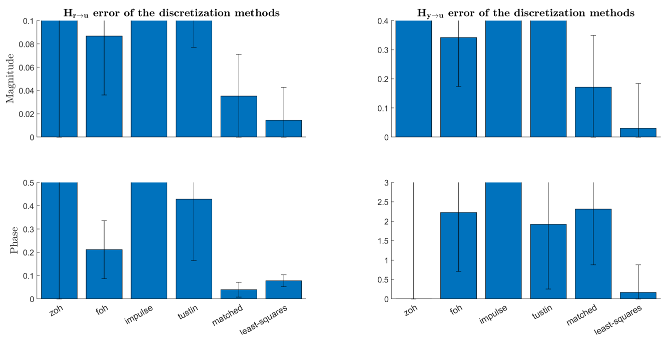

Fig. 13. Error of the different discretization methods with their standard deviation.

B. Results

Figure 14 shows the expected time response of different controllers. The figure shows a section of the sweep function between 10 and 10.5 seconds. This section corresponds to frequncies of around 10Hz. The first two signals correspond to the controller obtained with the optimization method (New) and what this signal should theoretically look like without any disturbance or delay (Ideal). It is shown that both signals are quite similar. The next signal is the one with the controller obtained using $\mathcal{H}_\infty$ synthesis (Prev). It can be seen that this controller performs worse in both amplitude and phase shift. The last controller that is evaluated is the controller obtained in this report but without the DOB, so, only a PD controller (PD). It can be seen that this is by far the worst performing controller. It also shows the clear benefits of adding a DOB.

Next, the results were analyzed in the frequncy domain. Figure 15 shows the different considered transfer functions. The first two functions are the controller obtained in this report (New) and it's ideal model (Ideal). It is shown that at low frequencies both functions are quite similar, however, at higher frequncies they vary significantly. A delay was added at the measurement of the ideal model (Delayed). The obtained function showed a shift in the resonance frequncy

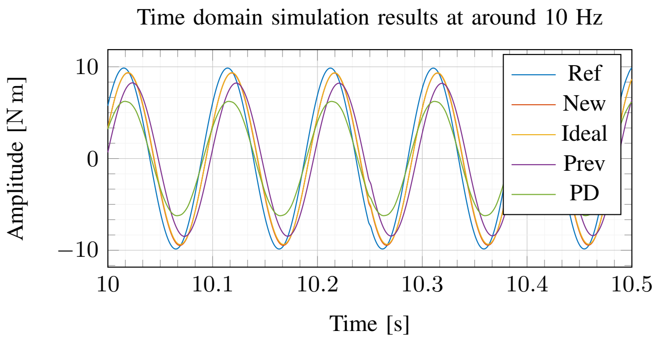

Fig. 14. Time response of different controllers.

and a large increase in it's magnitude. When the delay is considered in the ideal system, it approaches the frequency domain signal obtained in the simulations. This shows that, in this specific system, delay has a large impact and should be considered in the controller design. Next, the controller obtained using $\mathcal{H}_\infty$-synthesis was considered (Prev). It is shown that this controller has a weaker performance and struggles to compensate for the disturbances caused by the load inertia. Finally, the obtained controller was considered without the DOB (PD). It is shown that this controller performs poorly with the used load inertia. Comparing this performance with the one obtained using the DOB shows the effectiveness of the DOB.

The obtained controller shows better tracking capabilities than the controller obtained with $\mathcal{H}_\infty$-synthesis. The controll is sufficiently robust for the simulation preformed, which should be somewhat realistic. However, it should be tested in a real system to see if the performance changes. Finally, it was observed that the performance changes significaltly when delays are considered. Because of this, it may be beneficial to include delays in the optimization algorithm.

VII. Conclusion

The proposed method shows promising results, improving robustness while maintaining robustness. The controller design is written as an optimization problem. Even though the proposed system is relatively simple with two degrees of freedom, the same approach could be applied to more complex systems. On top of that, defining requirements as inequality constraints allows to implement them easily into the controller design. This approach also allows to easily implement time domain requirements which are complicated to implement in more traditional methods.

However, implementing new functions may not be as trivial as it may seem. This is because it has to be ensured first that the functions that will be used are continuous and so does it's gradient for the entire range to be considered. If this is not the case, the minimization algorithm will not work. On top of that, a deep understanding of the system is needed

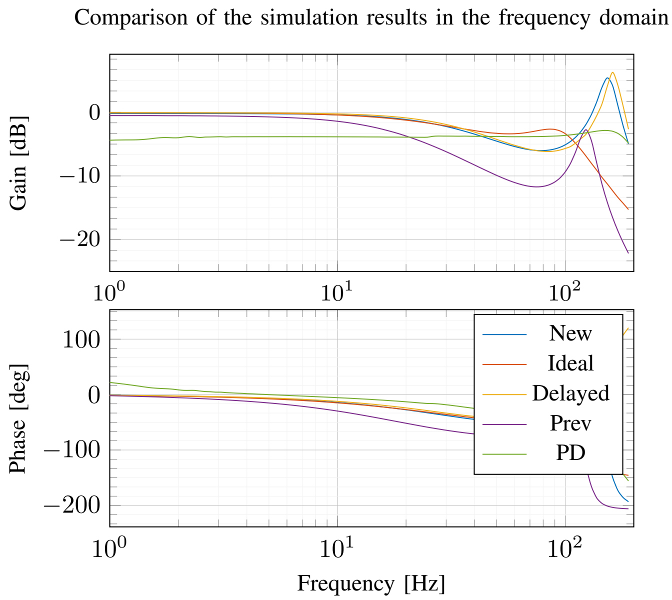

Fig. 15. Frequncy response of different controllers.

to select the appropriate functions. Finally, it is can not be ensured that the absolute minimum will be achieved and the output of the minimization ends at a local minimum.

In comparison with a controller obtained with traditinal $\mathcal{H}_\infty$ design, the obtained controller also showed both better performance and smaller variations caused by changes in the load inertias. This robustness to changes in load inertias makes the controller ideal for use in articulated robots. On top of that the transparency obtained with the DOB makes the system a good candidate to use in applications where humans are involved or in which the environment is unknown.

References

[1] Gill A Pratt and Matthew M Williamson. Series Elastic Actuators. pages 399–406, 1995.

[2] Jerry Pratt, Ben Krupp, and Chris Morse. Series elastic actuators for high fidelity force control. *Industrial Robot: An International Journal*, 29(3):234–241, 2002.

[3] Joshua S Mehling, James Holley, and Marcia K O'malley. Leveraging Disturbance Observer Based Torque Control for Improved Impedance Rendering with Series Elastic Actuators. Technical report, 2015.

[4] David W Robinson, Jerry E Pratt, Daniel J Paluska, and Gill A Pratt. Series Elastic Actuator Development for a Biomimetic Walking Robot. Technical report, 1999.

[5] Heike Vallery, Ralf Ekkelenkamp, Herman Van Der Kooij, and Martin Buss. Passive and Accurate Torque Control of Series Elastic Actuators. Technical report, 2007.

[6] Berno J E Misgeld, Anake Pomprapa, and Steffen Leonhardt. Robust control of compliant actuators using positive real H_2-controller synthesis. 2014.

[7] Nicholas Paine, Joshua S Mehling, James Holley, Nicolaus A Radford, Gwendolyn Johnson, Chien-Liang Fok, and Luis Sentis. Actuator Control for the NASA-JSC Valkyrie Humanoid Robot: A Decoupled Dynamics Approach for Torque Control of Series Elastic Robots. *Journal of Field Ronotics*, 00:1–19, 2015.

[8] Wesley Roozing and Gustavo A Medrano-cerda. Robust Disturbance Observer based Torque Control for Series-Elastic Actuators. pages 1–14, 2019.

[9] G Meinsma, H Kwakernaak, and O Bosgra. *Nine Lessons on Control Systems*. 2019.

[10] Emre Sariyildiz and Kouhei Ohnishi. A Guide to Design Disturbance Observer. *Journal of Dynamic Systems, Measurement and Control*, 136, 2014.

[11] Wesley Roozing, Jörn Malzahn, Darwin G Caldwell, and Nikos G Tsagarakis. Comparison of Open-Loop and Closed-Loop Disturbance Observers for Series Elastic Actuators. In *International Conference on Intelligent Robots and Systems*, pages 3842–3847, Daejeon, 2016.

[12] Sigurd Skogestad and Ian Postlethwaite. *Multivariable Feedback Control: Analysis and design*. Wiley, 2 edition, 2005.

[13] Stephen Boyd and Lieven Vandenberghe. *Convex Optimization*. 2004.

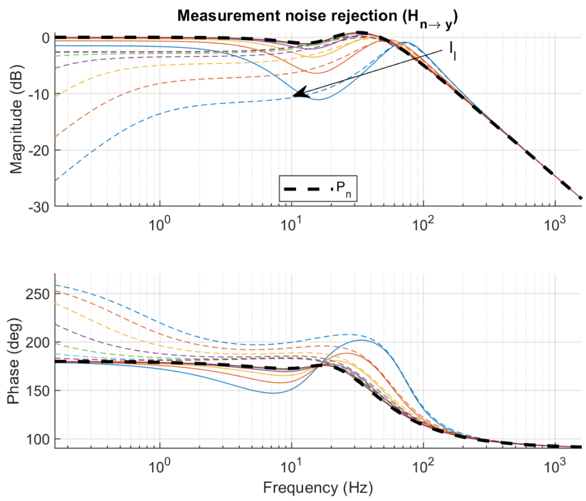

Figure 10: Noise rejection with DOB (continuous) and without DOB (dashed) compared to the nominal plant.

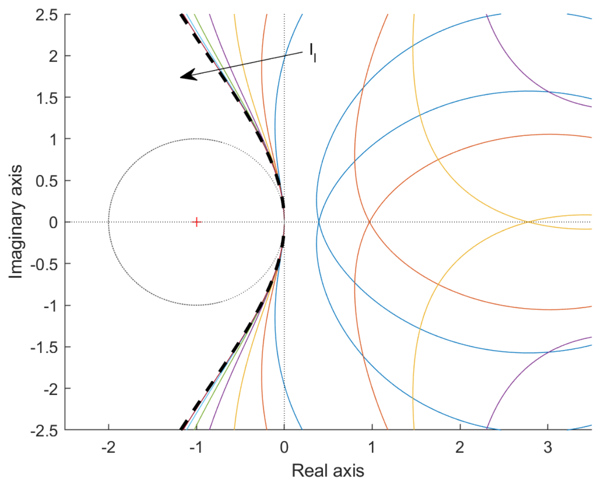

Figure 11: Nyquist plot of the system with DOB

3.2 μ-Synthesis

In the previous method, the PD controller was used to achieve the desired performance of the nominal plant and the DOB was used to achieve robustness to a range of load inertias. This method will be similar in that the same PD controller will be used to achieve the desired performance of the nominal plant and μ-sinthesis will be used to obtain a controller that has that colosed-loop performance with robustness to a range of load inertias and other disturbances.

Figure 12 shows the block diagram of the problem statement to obtain robust performance. There are three different inputs: The reference, r, is the signal that wants to be followed; the disturbance, d, represents any external disturbance and the noise, n, represents the measurement noise. There are two different outputs to be minimized: the error, e, is the error between the obtained output and the desired output, the controller output, u, is related to the work done by the controller. The different weight functions of the inputs (W_d, W_s and W_n) are used to specify the frequency content of the input signals. The weights on the output (W_e and W_u) are used to penalize some frequencies of the output signal. The weight function W_f is the desired closed-loop behavior of the system [11].

The diferent weight functions should be chosen as explained below:

- $\mathbf{W_d}$: The disturbances usually do not vary with frequency, however, if they do, that information can be added.
- $\mathbf{W_s}$: The reference usually does not vary with frequency, however, in some cases the expected reference is below

a specific frequency.

- $\mathbf{W_n}$: The noise is usually higher at higher frequencies.
- $\mathbf{W_f}$: The desired closed-loop performance will depend on the application.
- $\mathbf{W_e}$: The error weight is the inverse of the allowed magnitude of a specific error.
- $\mathbf{W_u}$: This function is usually small at zero frequency.

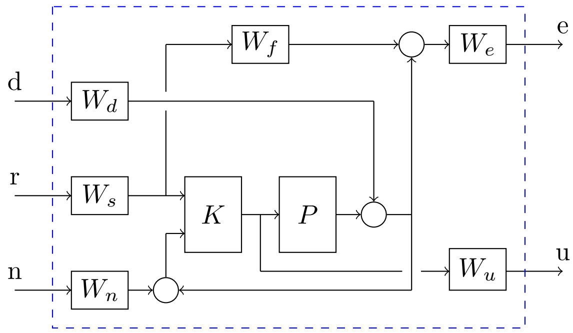

Figure 12: Block diagram for robust performance with μ-synthesis

This method does not take into account the delays that the system may have. Since the μ-synthesis method does not support time delays, its effect has to be approximated. This can be done by introducing a Padé approximation into the measured signal as shown in figure 13. This approximation models the phase shift caused by a time delay. It is accurate at lower frequencies and becomes inaccurate at higher frequencies, tending to a constant frequency shift. The frequency at which the approximation becomes inaccurate depends both on the time delay and the order of the approximation. The approximation should be accurate enough as soon as the frequencies of the delay margin are below this critical frequency [14]. The problem is that the frequency of the delay margin will depend on the controller, which, in turn, will depend on the Padé approximation used to derive it. So, it is not possible to know which order to use for the approximation. The best thing to do is to use a reasonable order to compute the controller and then check if the approximation holds for the frequency content of the closed-loop system. If it does not hold, try a higher order.

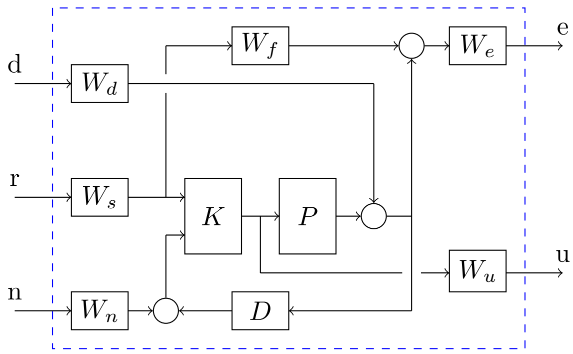

Figure 13: Block diagram for robust performance with μ-synthesis including delay.

Figure 14 shows the implementation of the block diagram to be used with MATLAB's command `musyn`. The model in figure 13 has to be modified to extract the controller. The modified plant includes the inputs and outputs shown in figure 12 and 13 plus the inputs and outputs of the controller. The inputs of the controller will become outputs of the modified plant and the outputs will be inputs. To make the model compatible with the `musyn` command, the inputs and outputs that connect with the controller have to be the last inputs or outputs.

Parameter		Value	
Gearbox ratio	n	80	
Torque constant	k_τ	0.078	[N m A^{-1}]
Rotor+gear inertia	I_m	0.295	[kg m^2]
Rotor+gear viscous	d_m	2.22	[N m s rad^{-1}]
Load viscous friction	d_l	0	[N m s rad^{-1}]
Rotor+gear Coulomb	$d_{c,m}$	3.54	[N m]
Load Coulomb friction	$d_{c,l}$	0	[N m]
Gear internal viscous	d_{mg}	80	[N m s rad^{-1}]
Sensor internal viscous	d_{gl}	0	[N m s rad^{-1}]
Gearbox stiffness	k_g	10^4	[N m rad^{-1}]
Sensor stiffness	k_b	5714	[N m rad^{-1}]

Table 1: Parameters used for the SEA model [8].

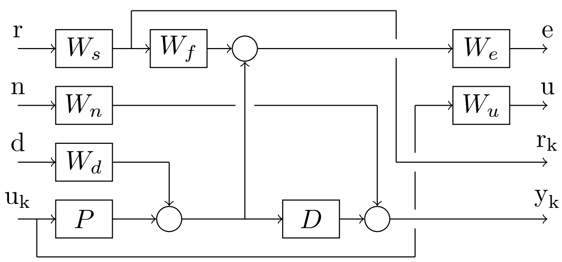

Figure 14: Block diagram for robust performance with μ-synthesis modified for use with the `musyn` command.

3.3 Implementation

The obtained controller will be compared with the controller obtained whith the $\mathcal{H}_\infty$ optimization. For that reason, the same model parameters as in [8] will be used. The parameters are shown in table 1. These parameters are based on the datasheet and parameter estimation of a real SEA.

The used weights are shown in figure 15. The ideal closed-loop response is set to be the closed loop response of the nominal plant in figure 3 with $K_p = 3$ and $K_d = 0.019$. The W_u should be used to limit the output of the controller so that it is applicable in the real system. However, no controller could be found with the control signal limited. This weight was set to 0. The resultant controller is likely to not work in a real system, since the actuator will not be able to deliver the required torques.

4 Analysis

The three different methods are compared in this section. The first controller is the one obtained with the $\mathcal{H}_\infty$ methods. The parameters used are $K_p = 3$, $K_d = 0.019$ and $\omega_c = 105.4$. The second method is the controller obtained in the optimization method, with the control parameters being $K_p = 10.25$, $K_d = 0.0365$ and $\omega_c = 596.34$. And the third controller is the one obtained using μ-synthesis, with the settings shown in section V. These controllers will be represented with a dashed, continuous and dotted line respectively. Besides that, the following plots show seven different inertias, logarithmically spaced between 0.04 and 10. Each inertia will be represented by a different color, which will be consistent throughout all the plots. Finally, the arrow will represent the direction that the plot tends to go with increasing load inertias. Large load inertias tend to approach the nominal case whereas smaller load inertias are larger disturbances.

Figure 16 shows the reference tracking. It is shown that, using the optimization method, a larger bandwidth is obtained. The controller obtained using μ-synthesis follows the closed-loop response of the nominal case for all the load inertias.

Figure 17 shows the disturbance rejection. It is shown that with the controller using the optimization, disturbance

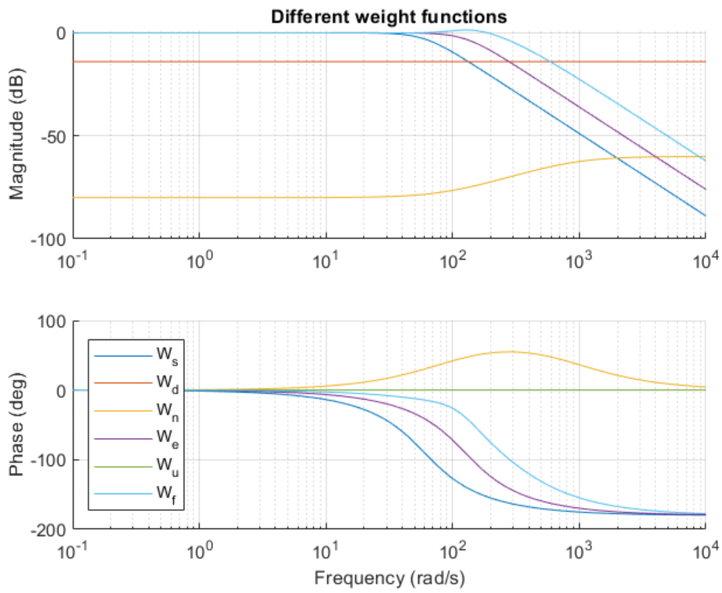

Figure 15: Weight functions used in μ-synthesis.

rejection is increased at lower frequencies. At higher frequencies, disturbance rejection is similar. With the controller obtained using μ-synthesis, disturbance rejection is greatly increased.

Figure 18 shows the noise rejection. It is shown that both controllers obtained with $\mathcal{H}_\infty$ and the optimization approach have similar noise rejection characteristics, whith the latter one being slightly worse at higher frequencies. The μ-sinthesis has the worst noise rejection capabilities. This is because of the large disturbance rejection, the controller is not capable of distinguishing between noise and a disturbance, it tries to compensate for the noise as if it were a disturbance and it passes it to the output.

5 Simulation

The simulation results obtained with the optimization method are shown in section VI of the self-sustained report.

The controller obtained using μ synthesis was unstable when implemented in the simulation. There are a few reasons that could make the system unstable. The first one that was considered is noise. As shown in figure 18, the noise rejection properties of the system are quite bad. In fact, the noise is let through to the output almost entirely for a large range of frequencies. However, measurement noise is unlikely to make the system unstable if it is not amplified. Another possible source of the instability is the control signal amplitude. If it is too large the signal would not pass through the limiter of the actuator and would not perform as expected, to the point that the system could become unstable. However, when the limiter was removed, the system remained unstable meaning that this is not what causes the instability, or, at least, not the only thing. The third thing that could cause the instability is related to the control signal's frequency content. Any control signal above the Nyquist frequency will not be reproducible. This could make the system unstable if high frequency signals are the primary control signals.

6 Discussion

In this report, two methods for designing torque controllers for SEAs were evaluated. The first discussed method defines the controller design as an optimization problem. This method was tested with the use of an example. It is shown that the method is viable, obtaining results with improved performance and which are robust to different disturbances applied in the simulation. However, this method should be tested in a real system as well.

A few different metrics are proposed in the report. However, many other metrics could have been used for both robustness and performance [11]. The decision of which functions to use will depend on the implementation and it's

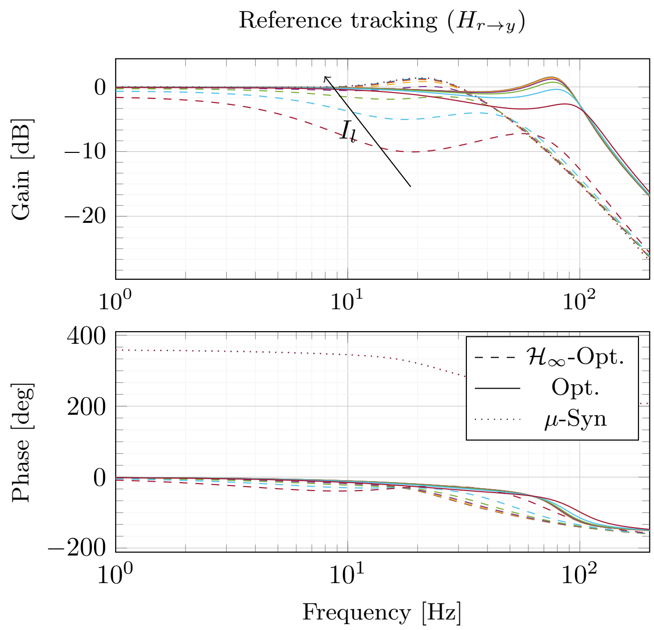

Figure 16: Comparison of the reference tracking with the different controllers.

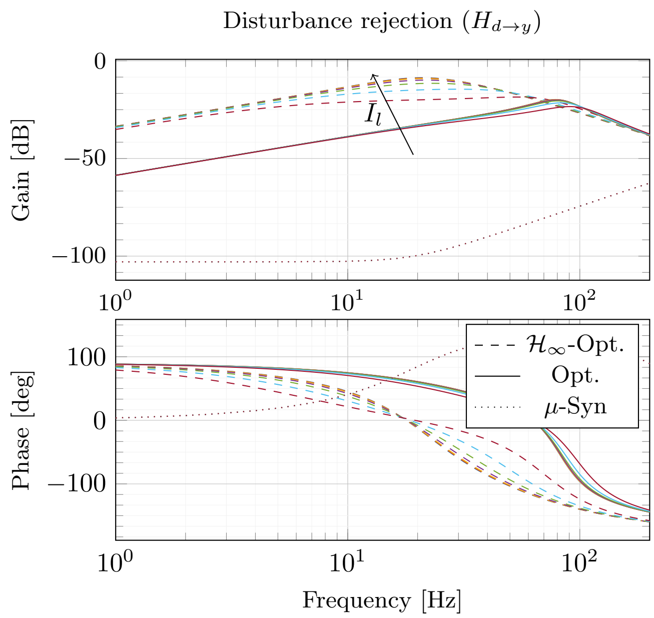

Figure 17: Comparison of the disturbance rejection with the different controllers.

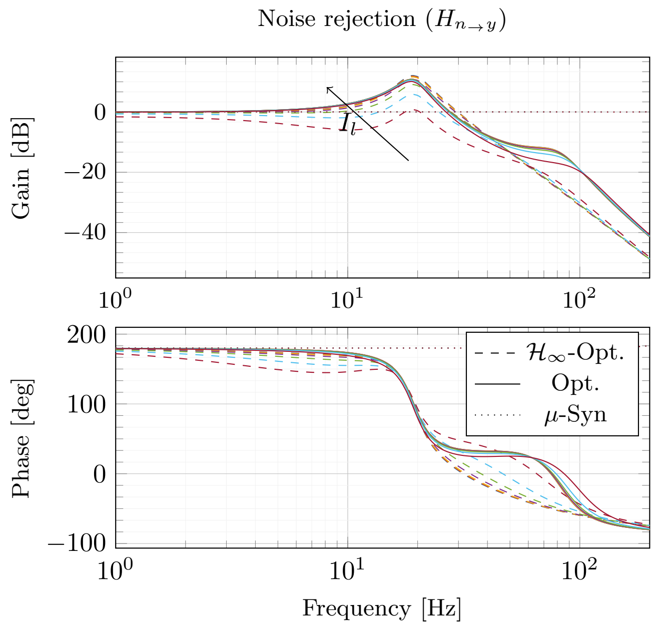

Figure 18: Comparison of the noise rejection with the different controllers.

objectives and requirements. It is important to ensure that the used metrics are constant and so is their gradient. If they are not, the optimization algorithm may not work as expected and the optimal controller may not be found [15].

It is important to note that convergence at the absolute minimum is not mathematically ensured. Based on extensive analysis of the used functions, it is believed that the absolute minimum will be found with almost any requirements that are set. However, the same cannot be said if an additional function is added. There are easy to apply methods to increase ones confidence of being at an absolute minimum, such as changing the initial conditions to see if the same optimal parameters are found. Further research should be done on different functions that one may want to implement in order to see which ones are less likely to produce local minima or not be valid at all.

While performing simulations, it was observed that the result of the reference tracking changed considerably with respect to the theoretical frequency response. This difference was attributed to the delay. When a delay is added, the resonance frequency of the reference tracking shifts and so does its gain. It was also noticed that the gain becomes finite. It is recommended that, in further work, the expected delay is added. The minimum allowed delay margin then could be decreased significantly. Considering the delay will ensure that the system remains stable and that the requirements are met.

The second method that was implemented uses μ-synthesis, a method to obtain controllers with robust performance without the overconservatism issues of $\mathcal{H}_\infty$ [16]. A PD controller is used to define the desired performance of the nominal plant and μ-synthesis is used to ensure robust performance for the considered range of inertias. A controller was obtained that showed promising results in the frequency domain analysis. However, when it was implemented in a realistic simulation, the system became unstable. Possible causes of this instability were discussed in section 5.

Even though no results were obtained with this method, it is believed that it could still be a viable solution. The method has been used before to solve the overconsrevatism of $\mathcal{H}_\infty$-synthesis [16]. The main problem is that weight selection requires a deep understanding of the method. Further research could find a systematic method for defining the different weight functions. There are also different ways of stating the synthesis problem that could prove better for the system.

7 Conclusion

In this report, two methods were proposed to reduced the overconservative obtained with the use of $\mathcal{H}_\infty$-synthesis in the tunning of a DOB based torque controller for a series elastic actuator. The first method states the controller design as an optimization problem. This method showed promising results, obtaining a controller with improved performance and which was robustly stable. The second method used a PD controller to define the desired closed-loop response of the nominal system μ-synthesis to ensure that the system was robustly stable to changes in the load inertia and other external disturbances. The controller showed promising results however, when implementing it in simulation the system became unstable. The most likely cause of this instability is the magnitude and frequency content of the control signal.

Stating the control design as an optimization function is easy to implement and was shown to solve the overconservatism. Different requirements can be implemented in both the frequency and time domain. This makes this approach an atractive option for controller design. However, when choosing the the functions to be used, it has to be ensured that they are continuous and so is their gradient. Convergence at the absolute minimum is also not ensured, so it will have to be evaluated in a case by case basis.

Using μ-synthesis for the controller design is a mathematically sound approach that, in theory, should solve the overconservatism issues that arise with the use of $\mathcal{H}_\infty$ optimization [16]. The method, however, is mathematically complex and weight selection requires a deep understanding of the method. A controller that has great disturbance rejection was obtained, however, it is not a viable controller due to the large and high frequency control signal.

It is proposed to use the μ-peak value as the objective function or a subfunction. By doing so, a μ-optimal controller could be obtained, ensuring robust performance with a mathematically sound theory and keeping the simplicity and versatility that the optimization method offers. Since more than one metric can be used in the optimization, the μ-peak value can be only calculated for the reference tracking. This would simplify the weigth selection process significantly.

The controller obtained with the optimization perform better than the one it was compared to, obtainde using $\mathcal{H}_\infty$-synthesis. The controller also showed greater robustness to changes in load inertias. This robustness makes the controller ideal for use in articulated robots. On top of that the transparency obtained with the DOB makes the system a good candidate to use in applications where humans are involved or in which the environment is unknown.

Bibliography

[1] Gill A Pratt and Matthew M Williamson. Series Elastic Actuators. pages 399–406, 1995.

[2] Jerry Pratt, Ben Krupp, and Chris Morse. Series elastic actuators for high fidelity force control. *Industrial Robot: An International Journal*, 29(3):234–241, 2002.

[3] Joshua S Mehling, James Holley, and Marcia K O'malley. Leveraging Disturbance Observer Based Torque Control for Improved Impedance Rendering with Series Elastic Actuators. Technical report, 2015.

[4] David W Robinson, Jerry E Pratt, Daniel J Paluska, and Gill A Pratt. Series Elastic Actuator Development for a Biomimetic Walking Robot. Technical report, 1999.

[5] Heike Vallery, Ralf Ekkelenkamp, Herman Van Der Kooij, and Martin Buss. Passive and Accurate Torque Control of Series Elastic Actuators. Technical report, 2007.

[6] Berno J E Misgeld, Anake Pomprapa, and Steffen Leonhardt. Robust control of compliant actuators using positive real H_2-controller synthesis. 2014.

[7] Nicholas Paine, Joshua S Mehling, James Holley, Nicolaus A Radford, Gwendolyn Johnson, Chien-Liang Fok, and Luis Sentis. Actuator Control for the NASA-JSC Valkyrie Humanoid Robot: A Decoupled Dynamics Approach for Torque Control of Series Elastic Robots. *Journal of Field Ronotics*, 00:1–19, 2015.

[8] Wesley Roozing and Gustavo A Medrano-cerda. Robust Disturbance Observer based Torque Control for Series-Elastic Actuators. pages 1–14, 2019.

[9] G Meinsma, H Kwakernaak, and O Bosgra. *Nine Lessons on Control Systems*. 2019.

[10] Joern Malzahn, Wesley Roozing, and Nikos Tsagarakis. The Compliant Joint Toolbox for MATLAB: An Introduction With Examples. *IEEE Robotics and Automation Magazine*, 26(3):52–63, 2019.

[11] Sigurd Skogestad and Ian Postlethwaite. *Multivariable Feedback Control: Analysis and design*. Wiley, 2 edition, 2005.

[12] Gary J Balas, John C Doyle, Keith Glover, Andy Packard, and Roy Smith. µ-Analysis and Synthesis Toolbox. Technical report, 1993.

[13] Kemin Zhou, John C Doyle, and Keith Glover. *Robust and Optimal Control*. Prentice hall, 1 edition, 1995.

[14] Song Zhang and Vijay Vittal. Design of wide-area damping control robust to transmission delay using μ-synthesis approach. In *IEEE Power and Energy Society General Meeting*, volume 2014-Octob. IEEE Computer Society, oct 2014.

[15] Stephen Boyd and Lieven Vandenberghe. *Convex Optimization*. 2004.

[16] Bilin Aksun Guvenq and Levent Guvenq. Robustness of Disturbance Observers in The Presence of Structured Real Parametric Uncertainty. Technical report, 2001.